JAERI-M
88-095

ENERGY CONFINEMENT STUDY IN JT-60 INITIAL HEATING EXPERIMENT

May 1988

Nobuyuki HOSOGANE, Masato AKIBA, Masaaki KURIYAMA
Naoyuki MIYA, Kenkichi USHIGUSA, Ryuji YOSHINO
and Hiromasa NINOMIYA

日本原子力研究所
Japan Atomic Energy Research Institute

JAERI-M レポートは，日本原子力研究所が不定期に公刊している研究報告書です。
入手の問合わせは，日本原子力研究所技術情報部情報資料課（〒319－11 茨城県那珂郡東海村）あて，お申しこしください。なお，このほかに財団法人原子力弘済会資料センター（〒319-11 茨城県那珂郡東海村日本原子力研究所内）で複写による実費頒布をおこなっております。

JAERI-M reports are issued irregularly.
Inquiries about availability of the reports should be addressed to Information Division, Department of Technical Information, Japan Atomic Energy Research Institute, Tokai-mura, Naka-gun, Ibaraki-ken 319-11, Japan.

編集兼発行　日本原子力研究所
印　　刷　山田軽印刷所

JAERI-M 88-095

Energy confinement study in JT-60 initial heating experiment

Nobuyuki HOSOGANE, Masato AKIBA[+], Masaaki KURIYAMA[+]
Naoyuki MIYA, Kenkichi USHIGUSA, Ryuji YOSHINO
and Hiromasa NINOMIYA

Department of Large Tokamak Research
Naka Fusion Research Establishment
Japan Atomic Energy Research Institute
Naka-machi, Naka-gun, Ibaraki-ken

(Received April 27, 1988)

Parameter dependences of energy confinement time are investigated of the JT-60 divertor plasmas heated by the hydrogen neutral beam with power up to 20 MW. The experimental data obtained under the low radiation level less than about 10% of the absorbed power are used to investigate the following parameter dependences; (1) absorbed power (P_{abs}), (2) beam energy, (3) co- and counter- injection, (4) electron density ($\bar{n}_e$), (5) plasma current (I_p) and (6) safety factor (q_{eff}). With these parameter dependences, scaling laws of the JT-60 divertor plasmas are drawn as follows;

$$\tau_E^s(\mathrm{sec}) = (0.033 + 0.37/P_{abs}(\mathrm{MW})) \times I_p^{0.6}(\mathrm{MA}) \bar{n}_e^{0.14}(10^{19}\mathrm{m}^{-3}) q_{eff}^{0},$$

or

$$\tau_E^s(\mathrm{sec}) = 0.26 P_{abs}(\mathrm{MW})^{-0.56} \times I_p^{0.6}(\mathrm{MA}) \bar{n}_e^{0.14}(10^{19}\mathrm{m}^{-3}) q_{eff}^{0}.$$

Keywords: JT-60, Divertor, Parameter Dependence, Energy Confinement, Scaling

---

+ Department of JT-60 Facility

JT－60の初期加熱実験におけるエネルギー閉込めの研究

日本原子力研究所那珂研究所臨界プラズマ研究部
細金延幸・秋場正人[+]・栗山正明[+]・宮　直之
牛草健吉・茅野隆治・二宮博正

（1988年4月27日受理）

20 MWまでの水素原子を使った中性粒子加熱を行った場合のJT－60ダイバータプラズマのエネルギー閉込め時間について，パラメータ依存性を調べた。放射損失が10%以下という低放射損失レベルのプラズマで得たデータを使用し，以下の依存性を調べた：(1) 吸収パワー，(2) ビームエネルギー，(3) co－/counter －入射，(4) 電子密度，(5) プラズマ電流，(6) 安全係数。これらの依存性を使い，次のようなJT－60の閉込め時間のスケーリング則を求めた。

$$\tau_E^S = (0.033 + 0.37/\mathrm{Pabs\ (MW)}) \times I_P^{0.6}\ (\mathrm{MA})\ \bar{n}_e^{0.14}\ (10^{19}\,\mathrm{m^{-3}})\ q_{eff}^{0}\ (\mathrm{sec})$$

又は，

$$\tau_E^S = 0.26\ \mathrm{Pabs}^{-0.56}\ I_P^{0.6}\ (\mathrm{MA})\ \bar{n}_e^{0.14}\ (10^{19}\,\mathrm{m^{-3}})\ q_{eff}^{0}\ (\mathrm{sec})$$

那珂研究所：〒311-01　茨城県那珂郡那珂町大字向山801－1
＋　JT－60試験部

Contents

目　　次

1. Introduction

Scaling laws of energy confinement time of auxiliary heated plasma are important and useful not only for understanding confinement characteristics of plasmas but also for designing a new machine such as next generation tokamaks. So far, some scaling laws have been studied with using experimental data obtained in small and medium tokamaks [1,2,3], and have often been used to evaluate a standard energy confinement time to be compared with new experimental results. Recently, high power heating experiments have been performed in large tokamaks, TFTR[4], JET[5] and JT-60[6,7]. To obtain more reliable scaling laws, it is necessary to investigate their parameter dependences of energy confinement time, and to reconstruct new scaling laws with using these experimental results.

JT-60 is a large tokamak with a compact poloidal divertor at the outside of the torus[6], the first walls of which consist of the TiC-coated molybdenum limiters and divertor plates. The neutral beam heating experiments in JT-60 have been performed with the divertor plasmas mainly in the high power region above 10 MW. Because of the effective reduction of impurity influx by the divertor action, the heating experiments with very low radiation loss (less than 10% of the injected power) was successfully performed in the wide parameter region. The results obtained in JT-60 under these low radiation level will offer an reliable input to the database for reconstructing a new scaling law.

In this paper, the parameter dependences of energy confinement time in JT-60 divertor plasma is presented, each of which is compared with a conventional scaling law (the Goldston scaling law). As a summary, a scaling law in JT-60 is drawn by using these parameter dependences.

2. Operation and Operational Parameter Region

Confinement characteristics of the neutral beam heating were mainly investigated in the divertor plasmas. The operation parameters are summarized in Table 1. The parameter, δ_{30}, is a clearance between the plasma surface and the limiter at a poloidal angle of 30 degrees in the divertor equilibria[6], which is controlled to maintain the divertor action during the heating. As a result of the divertor control, Z_{eff}, was reduced to 1-2 in the electron density of $2\text{-}7\times10^{19}$ m^{-3}. The radiation loss was suppressed to less than about 10% of the absorbed power in the divertor plasmas, while in the limiter plasmas it reached 50-80%[6].

Neutral beam lines are almost perpendicular to the axis of plasma column (78 degrees). The ratio of co- and counter-injection is usually 8:6. The hydrogen neutral beam was injected not only into hydrogen plasmas but also into helium plasmas. The neutral beam heating region for each plasma is shown in Fig. 1. To obtain high absorption power even in the low electron density region, helium plasmas were mainly used in the experiment with

In this paper, the parameter dependences of energy confinement time in JT-60 divertor plasma is presented, each of which is compared with a conventional scaling law (the Goldston scaling law). As a summary, a scaling law in JT-60 is drawn by using these parameter dependences.

2. Operation and Operational Parameter Region

Confinement characteristics of the neutral beam heating were mainly investigated in the divertor plasmas. The operation parameters are summarized in Table 1. The parameter, δ_{30}, is a clearance between the plasma surface and the limiter at a poloidal angle of 30 degrees in the divertor equilibria[6], which is controlled to maintain the divertor action during the heating. As a result of the divertor control, Z_{eff}, was reduced to 1-2 in the electron density of $2\text{-}7\times10^{19}$ m^{-3}. The radiation loss was suppressed to less than about 10% of the absorbed power in the divertor plasmas, while in the limiter plasmas it reached 50-80%[6].

Neutral beam lines are almost perpendicular to the axis of plasma column (78 degrees). The ratio of co- and counter-injection is usually 8:6. The hydrogen neutral beam was injected not only into hydrogen plasmas but also into helium plasmas. The neutral beam heating region for each plasma is shown in Fig. 1. To obtain high absorption power even in the low electron density region, helium plasmas were mainly used in the experiment with

$\bar{n}_e \leq 3\times10^{19}$ m^{-3} because the ionization rate of the neutral beam by helium plasma is higher than that by hydrogen plasma. Here, the ratio of hydrogen and helium atoms in this 'helium plasmas' is roughly estimated as 1:1 from the comparison of the intensities of H_α, the charge exchange neutral flux, etc. between hydrogen plasmas and 'helium plasmas'.

3. Stored Energy

The stored energy of heated plasma is calculated by using the following relation;

$$W^* = W_{OH} + 3/2(B_p^2/2\mu_0)\Delta(\beta_p + \ell_i/2)V_0 \quad (1)$$

Here, W_{OH} is a stored energy of ohmic plasma just before the heating. The empirical scaling law of the stored energy for JT-60 ohmic plasmas obtained by kinetic analysis[7],

$$W_{OH}(MJ) = 0.157 \times I_p^{0.86}(MA)\bar{n}_e^{-0.62}(10^{19}\ m^{-3}) \quad (2)$$

is used for the calculation of the ohmic stored energy. The second term in Eq.(1) is the incremental stored energy by the neutral beam heating, which is calculated by using the increment of Shafranov lambda, $\Delta(\beta_p + \ell_i/2)$, obtained in the equilibrium analysis, assuming that the change in internal inductance, li, during the heating is negligible. V_0 is the plasma volume. It

$\bar{n}_e \leqq 3\times10^{19}$ m^{-3} because the ionization rate of the neutral beam by helium plasma is higher than that by hydrogen plasma. Here, the ratio of hydrogen and helium atoms in this 'helium plasmas' is roughly estimated as 1:1 from the comparison of the intensities of H_α, the charge exchange neutral flux, etc. between hydrogen plasmas and 'helium plasmas'.

3. Stored Energy

The stored energy of heated plasma is calculated by using the following relation;

$$W^* = W_{OH} + 3/2(B_p^2/2\mu_0)\Delta(\beta_p + \ell_i/2)V_0 \quad (1)$$

Here, W_{OH} is a stored energy of ohmic plasma just before the heating. The empirical scaling law of the stored energy for JT-60 ohmic plasmas obtained by kinetic analysis[7],

$$W_{OH}(MJ) = 0.157 \times I_p^{0.86}(MA)\bar{n}_e^{-0.62}(10^{19}\ m^{-3}) \quad (2)$$

is used for the calculation of the ohmic stored energy. The second term in Eq.(1) is the incremental stored energy by the neutral beam heating, which is calculated by using the increment of Shafranov lambda, $\Delta\ (\beta_p + \ell_i/2)$, obtained in the equilibrium analysis, assuming that the change in internal inductance, li, during the heating is negligible. V_0 is the plasma volume. It

is noted that since $\beta_p = 1/2(P_\perp + P_\parallel)/(B_p^2/2\mu_0)$ [8], the stored energy, W*, becomes smaller than the ture value by $\delta(\Delta W^*) = 1/2 (W_\perp - W_\parallel)$ in the anisotropic equilibrium. However, according to the analysis of the slowing down process of fast ions with the Monte-Carlo method, the deviation $\delta(\Delta W^*)$, due to the anisotropy of the beam energy component is less than 7% at $\bar{n}_e = 2\times10^{19}$ m^{-3}, and decreases as the electron density increases. Hence, in the following investigations, no correction is made to the stored energy.

Figure 2 shows the stored energies, W*, against the absorbed power, $P_{abs} = P_{OH} + P_{abs}^{inj}$. The difference in stored energies between hydrogen plasmas and helium plasmas is not clear within the scatter of the data. It is probably due to the fact that the ratio of hydrogen and helium atoms in the "helium plasmas" is $H^+:He^{++} \fallingdotseq 1:1$, or there might be no mass dependence between these species. Therefore, both of data are used for investigating the parameter dependences of energy confinement time without classifying the operation gases.

4. Parameter Dependences of Energy Confinement Time

4.1 Absorbed power dependence

Figure 3 shows the absorbed power dependence of energy confinement time τ_E^*. Here, τ_E^* is defined as $\tau_E^* = W^*/P_{abs}$. As shown in Fig. 3, the absorbed power dependence can be expressed in the forms of $f(I_p, \bar{n}_e, \ldots)(a + b/P_{abs})$ or $f(I_p, \bar{n}_e \ldots) P_{abs}^x$.

is noted that since $\beta_p = 1/2(P_\perp + P_\parallel)/(B_p^2/2\mu_0)$ [8], the stored energy, W*, becomes smaller than the ture value by $\delta(\Delta W^*) = 1/2 (W_\perp - W_\parallel)$ in the anisotropic equilibrium. However, according to the analysis of the slowing down process of fast ions with the Monte-Carlo method, the deviation $\delta(\Delta W^*)$, due to the anisotropy of the beam energy component is less than 7% at $\bar{n}_e = 2\times10^{19}$ m^{-3}, and decreases as the electron density increases. Hence, in the following investigations, no correction is made to the stored energy.

Figure 2 shows the stored energies, W*, against the absorbed power, $P_{abs} = P_{OH} + P_{abs}^{inj}$. The difference in stored energies between hydrogen plasmas and helium plasmas is not clear within the scatter of the data. It is probably due to the fact that the ratio of hydrogen and helium atoms in the "helium plasmas" is $H^+ : He^{++} \fallingdotseq 1:1$, or there might be no mass dependence between these species. Therefore, both of data are used for investigating the parameter dependences of energy confinement time without classifying the operation gases.

4. Parameter Dependences of Energy Confinement Time

4.1 Absorbed power dependence

Figure 3 shows the absorbed power dependence of energy confinement time τ_E^*. Here, τ_E^* is defined as $\tau_E^* = W^*/P_{abs}$. As shown in Fig. 3, the absorbed power dependence can be expressed in the forms of $f(I_p, \bar{n}_e, \ldots)(a + b/P_{abs})$ or $f(I_p, \bar{n}_e \ldots) P_{abs}^x$.

Incorporating other parameter dependences, f, described in the following sections, a regression analysis gives a=0.033, b=0.37 or x=-0.56. Both functions fit the experimental data equally well within their statistical accuracy.

4.2 Beam energy and co-/counter-injection dependence

Figure 4 shows the beam energy dependence of energy confinement time. The dependence is investigated in the comparatively low power region of P_{abs}=9.3-11.4 MW because the maximum injection power decreases with beam energy (P_{abs}^{MAX}=13MW at E_b=50keV). The energy confinement time has a weak dependence on the electron density, but is independent of the beam energy in this power region.

Since most of the heating experiments were performed with the ratio of co- and counter-injection, 8:6, the detailed dependence of energy confinement time against the ratio of co- and counter-injection was not obtained. However, to investigate the effect of the direction of the beam injection, the following experiments were performed for co-injection alone and counter-injection alone, resectively.

(a) I_p = 1.5 MA, B_T=4.5 Tesla, $\bar{n}_e$=4.3-4.5×10^{19} m^{-3}, E_b=70 keV for P_{inj}^{co}, $P_{inj}^{counter}$=9.1 MW

(b) I_p = 1.2 MA, B_T = 2.75 Tesla, $\bar{n}_e$ = 2.1-2.3×10^{19} m^{-3}, E_b=70 keV for P_{inj}^{co}, $P_{inj}^{counter}$=4.5 MW

In both experiments, almost the same energy confinement times

were obtained for the respective injection (τ_E^* = 124 msec for co-injection, 122 msec for counter-injection in (a) and τ_E^*=123 msec for co-injection, 121 msec for counter-injection in (b)). As shown in Fig. 3, the energy confinement times obtained in the experiment (a) (symbol ☆ , ★) are almost same as those obtained in the experiment with both injections. According to the orbit analysis with Monte-Carlo method, the orbit loss for co- and counter-injection under the condition of I_p=1 MA and $\bar{n}_e$=3×10^{19} m^{-3} is 1% and 3%, respectively. From these experimental and numerical results, it is considered that there is no clear dependence on the direction of beam injection.

Thesefore, no classification with beam energy and injection direction is made in the following investigation.

4.3 Electron density dependence

Figure 5 shows the electron density dependence of the energy confinement time of 1.5 MA and 2 MA divertor plasmas. It is found that the energy confinement time of the divertor plasmas has a very weak dependence on the electron density like a function of $\bar{n}_e^{0.12\sim0.18}$, which is independent of the region of the absorbed power and the plasma current. If the correction of the anisotropic beam stored energy is made to the total stored energies of plasmas in the low electron density region, this dependence will become weaker. Thus, the electron density dependence of the JT-60 divertor plasma is almost same as the Goldston scaling law ($\propto \bar{n}_e^0$). This result implies that the stored

energy, W*, including beam stored energy is almost independent of electron density at the fixed absorbed power. Since the beam energy decreases with increase in electron density, the variation of electron temperataure is weaker than $1/\bar{n}_e$, which is consistent with the measurement of electron temperature in JT-60.

4.4 Plasma current dependence

Figure 6 shows the plasma current dependence of the energy confinement time. Since there is no common region of the electron density and the absorbed power from 1 MA plasmas to 2 MA plasmas, this dependence is investigated by deviding these parameters into several region as shown in Fig. 6. From this figure, the plasma current dependence of $I_p^{0.56-0.75}$ is obtained. Taking account of the correction of the beam stored energy to the 1 MA plasmas with low electron density, it may be considered that this dependence is approximately $I_p^{0.6}$.

Compared with the Goldston scaling law and the Kaye-Goldston scaling law[2] with strong dependence on plasma current ($\propto I_p$ and $I_p^{1.24}$, respectively), the JT-60 divertor plasma has a comparatively weak dependence on plasma current. The conventional scaling laws have been drawn with using the experimental results from limiter plasmas and divertor plasmas with a stangnation point at the top and/or the bottom of the torus. While, the JT-60 divertor plasma has a stagnation point at the outside of the torus. This difference might affect the current dependence of energy confinement time. The comparison of the results from the

divertor plasmas and the limiter plasmas in JT-60 will be an answer to this question. As shown in Fig. 6, the current dependence of the energy confinement time for the limiter plasmas is almost same as that for the divertor plasmas. However, it should be noted that the radiation level is very high in the neutral beam heating of the limiter plasmas as described above. Also, the energy confinement time of the limiter plasmas is worse than that of the divertor plasma. Taking account of this fact, to answer this question, it is necessary to compare the results obtained under the same level of the radiation loss.

4.5 Safety factor dependence

Figure 7 shows the safety factor dependence of energy confinement time. Here, a safety factor, q_{eff}, is defined as

$$q_{eff} = 2\pi a_p^2 B_T/\mu_0 \, RI_p(1 + (a_p/R)^2(1+(\beta_p+\ell_i/2)^2/2)).$$

To exclude the dependences on both the major and the minor radii, R and a_p, they were fixed almost constant, R=3.10-3.15 m and a_p=0.82-0.88 m in this experiment. The q_{eff} dependence was investigated by scanning the strength of the toroidal magnetic field from 1.9 Tesla to 4.5 Tesla for 1 MA plasmas and from 3.5 Tesla to 4.5 Tesla for 1.5 MA plasmas. From this figure, it is found that there is no q_{eff} dependence in the energy confinement time.

5. Scaling Law of Energy Confinement Time of the JT-60 Divertor Plasma

From the parameter dependences described above, scaling laws of energy confinement time of the JT-60 divertor plasma may be expressed by the following type functions;

$$\tau_E^s(\mathrm{sec}) = (a + b/P_{abs}(\mathrm{MW}))I_p^{0.6}(\mathrm{MA})n_e^{-0.14}(10^{19}\ \mathrm{m}^{-3})\ q_{eff}^{\circ},$$

or

$$\tau_E^s(\mathrm{sec}) = c\ P_{abs}(\mathrm{MW})^x I_p^{0.5}(\mathrm{MA})n_e^{-0.14}(10^{19}\ \mathrm{m}^{-3})\ q_{eff}^{\circ}\ .$$

Here, the coefficients, a, b, c and x obtained by regression analysis are a=0.033 and b=0.37, or c=0.26 and x=-0.56. Figures 8(a) and (b) show the comparisons of energy confinement times obtained in the experiment, τ_E^*, and those evaluated by the scaling law drawn above, τ_E^s, for the respective scaling laws. Both scalings fit the experimental data equally well within the same statistical accuracy, although their dependences on absorbed power are different. Within the data obtained in this experiment, it is difficult to determine which dependence is better.

In this experiment, the dependence on the plasma size (major and minor radii, R and a_p) was not investigated. To compare the JT-60 divertor results with the results of other tokamaks, the comparison of the energy confinement time of the JT-60 divertor plasma is made with that of the Goldston scaling law;

$$\tau_E^{GS}(\text{sec}) = 0.0368 I_p(\text{MA}) P_{abs}^{-0.5}(\text{MW}) R^{1.75}(\text{m}) a_p^{-0.37}(\text{m})$$

Since the energy confinement time depends on plasma current, the comparison is made in the following cases.

Case 1: I_p=2 MA, $\bar{n}_e$=4×10^{19} m^{-3}, P_{abs}=20 MW, R=3.15 m and a_p=0.83 m; τ_E^S=98 msec, τ_E^{GS}=133 msec.

Case 2: I_p=1 MA, $\bar{n}_e$=2×10^{19} m^{-3}, P_{abs}=20 MW, R=3.15 m and a_p=0.83 m; τ_E^S=54 msec, τ_E^{GS}=66 msec.

Here, it is noted that the Goldston scaling law is drawn with using the deuterium plasma data, while the JT-60 results are obtained with the hydrogen plasmas. In ASDEX[10], the mass dependence like $\tau_E^H = \tau_E^D \sqrt{m_H/m_D}$ has been obtained between hydrogen plasmas and deuterium plasmas. Here, τ_E^H and τ_E^D are the energy confinement time of hydrogen plasmas and deuterium plasmas, and m_H and m_D are the mass of hydrogen atom and deuterium atom. Assuming this mass dependence, the energy confinement time for the 2 MA plasma (Case 1) and the 1 MA plasma (Case 2) predicted by the Goldston scaling law become 93 msec and 46 msec, respectively. The JT-60 results for the 2 MA plasmas are almost same as the estimated value by the Goldston scaling law, but those for the 1 MA plasmas are slightly longer.

6. Summary

The parameter dependences of energy confinement time of JT-60 divertor plasma is investigated with using experimental data obtained in the high power neutral beam heating up to 20 MW under the significant feature of low radiation loss. The parameter dependences are summarized as scaling laws like following functions;

$$\tau_E^S(\mathrm{sec}) = (0.033 + 0.37/P_{abs}(\mathrm{MW})) \times I_p^{0.6}(\mathrm{MA}) n_e^{-0.14}(10^{19}\ \mathrm{m}^{-3}) q_{eff}^0,$$

or

$$\tau_E^S(\mathrm{sec}) = (0.26\ P_{abs}(\mathrm{MW}))^{-0.56} \times I_p^{0.6}(\mathrm{MA}) n_e^{-0.14}(10^{19}\ \mathrm{m}^{-3}) q_{eff}^0,$$

and are summarized as follows.

(1) Both type functions of $a + b/P_{abs}$ and P_{abs}^x fit the absorbed power dependence equally within the same statistical accuracy.

(2) The plasma current dependence is weaker than the conventional scaling laws such as Goldston scaling law[1,2,3].

(3) The electron density dependence is very weak.

(4) The beam energy dependence is not found in the region of E_b=50-75 keV, and no difference in energy confinement time is found between the co-injection and the counter-injection from a limited database.

(5) There is no q_{eff} dependence.

Acknowledgement

The authors would like to acknowledge Drs. Y. Shimomura and M. Nagami for their fruitful discussions. The authors would also like to acknowledge the JT-60 team who have contributed to this project, and Drs. S. Mori, K. Tomabechi, and M. Yoshikawa for their continued leadership and support.

References

[1] R.J. Goldston, Plasma Phys. and Cont. Fusion, 26(1984)87.

[2] S.M. Kaye and R.J. Goldston, Nuclear Fusion, 25(1985)65.

[3] T. Ohkawa, R.D. Stambaugh, and the Doublet III Physics Group, Plasma Phys. and Cont. Fusion, 28(1986)219.

[4] R.J. Hawryluk, et al., in Plasma Physics and Controlled Nuclear Fusion Research 1986 (Proc. 11th Int. Conf. Kyoto, 1986) Vol. 1, IAEA, Vienna, (1987)51.

[5] JET TEAM, in Plasma Physics and Controlled Nuclear Fusion Research 1986 (Proc. 11th Int. Conf. Kyoto, 1986) Vol. 1, IAEA, Vienna, (1987)31.

[6] JT-60 TEAM, in Plasma Physics and Controlled Nuclear Fusion Research 1986 (Proc. 11th Int. Conf. Kyoto, 1986) Vol. 1, IAEA, Vienna, (1987)11.

[7] JT-60 TEAM, in Plasma Physics and Controlled Nuclear Fusion Research 1986 (Proc. 11th Int. Conf. Kyoto, 1986) Vol. 1, IAEA, Vienna, (1987)89.

[8] M. Kikuchi, T. Hirayama, K. Shimizu, H. Yoshida, et al., Nuclear Fusion, 27(1987)1239.

[9] W.A. Cooper and A.J. Wootton, Plasma Physics, 24(1982)1183.

[10] F. Wagner, G. Becker, K. Behringer, D. Campbell, A. Eberhagen, et al., in Plasma Physics and Controlled Nuclear Fusion Research 1982 (Proc. 9th Int. Conf. Baltimore, 1982) Vol. 1, IAEA, Vienna (1982)43.

Table 1 Operational parameter region of neutral beam heating

Parameters	Range
Configuration	Divertor
I_p	1.0 - 2.0 MA
$\bar{n}_e$	$0.65\text{-}6.7\times10^{19}\,m^{-3}$
B_T	1.9 - 4.5 T
q_{eff}	2.2 - 6.2
R_p	3.09 - 3.15 m
a_p	0.82 - 0.91 m
δ_{30}	0.2 - 5.1 cm
Plasma gas	H_2 / He
P_{inj}	4 - 20 MW
E_{beam}	50 - 75 keV
$P_{co-}/(P_{co-}+P_{ctr})$	0 - 1

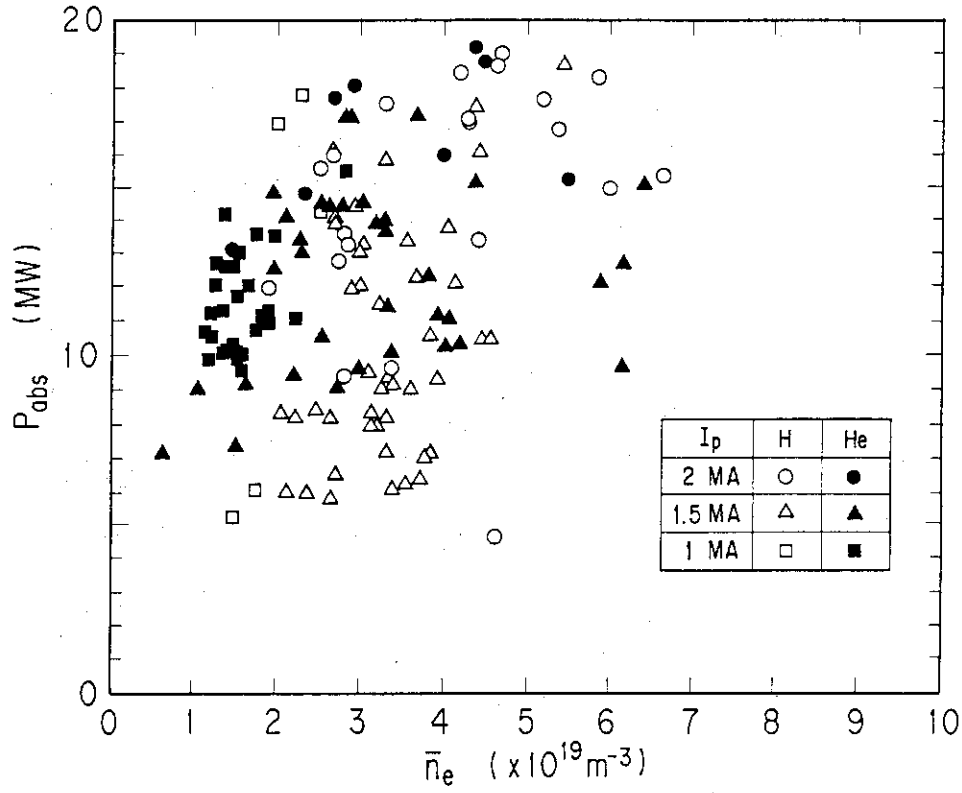

Fig. 1 Operation region of heating power and electron density.

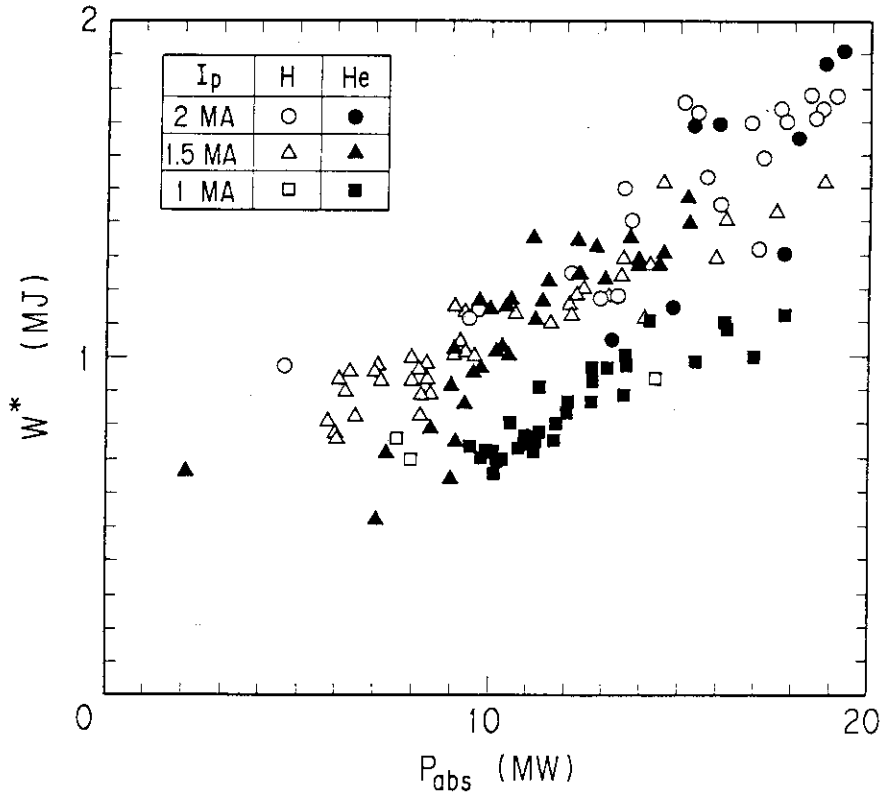

Fig. 2 Magnetically measured stored energy for divertor plasmas.

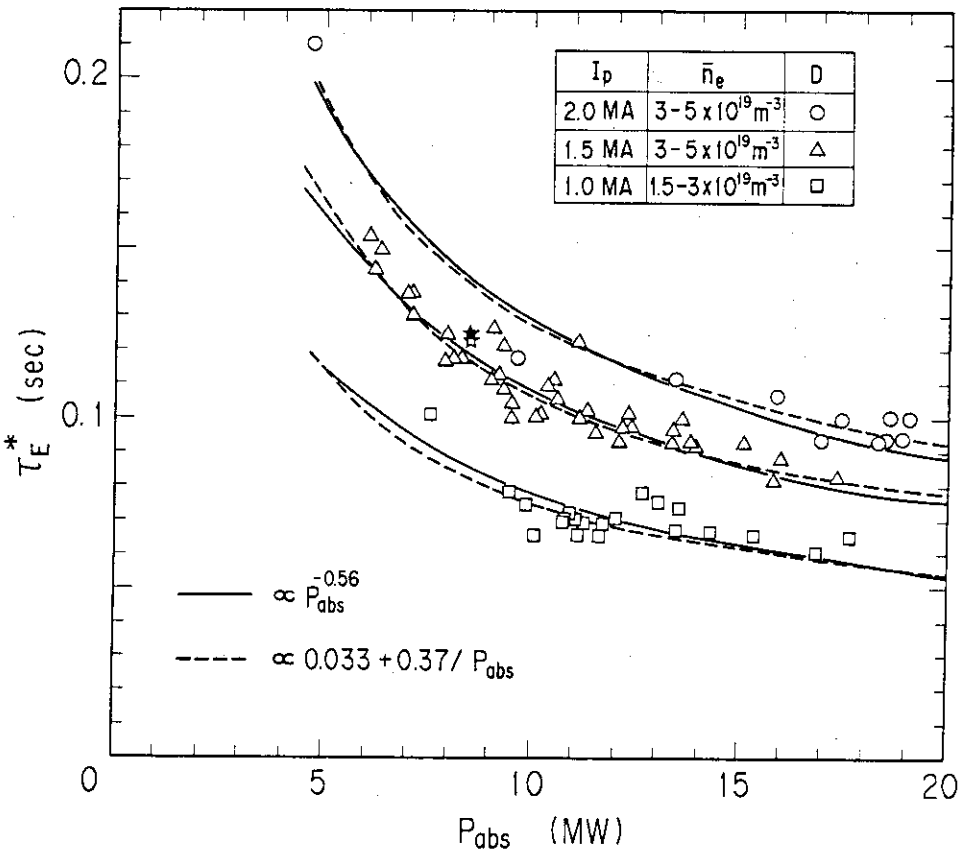

Fig. 3 Absorbed power dependence of energy confinement time, Symbols, ☆, ★ , show the results obtained in the experiments with co-injection alone and counter-injection alone, respectively.

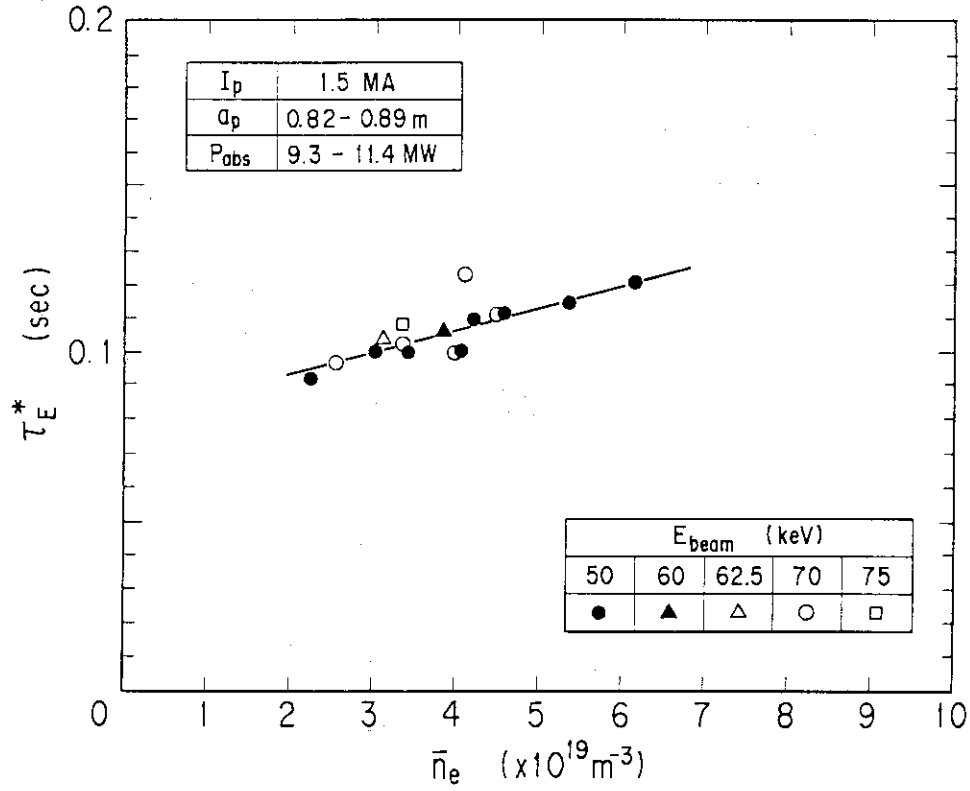

Fig. 4 Beam energy dependence of energy confinement time.

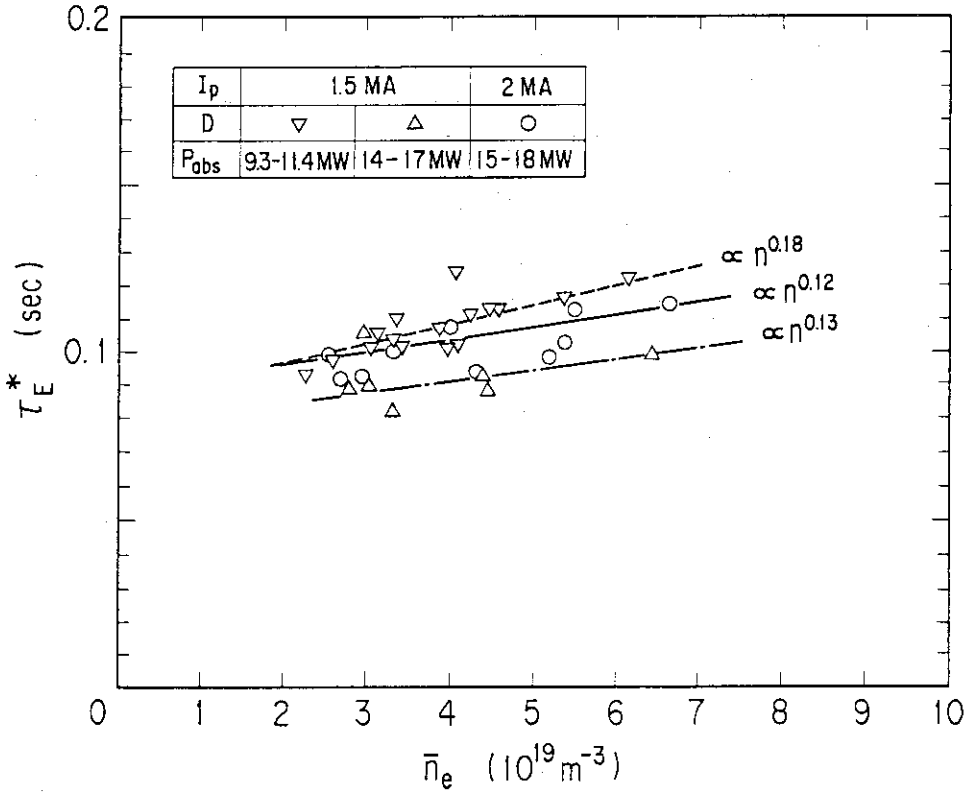

Fig. 5 Electron density dependence of energy confinement time.

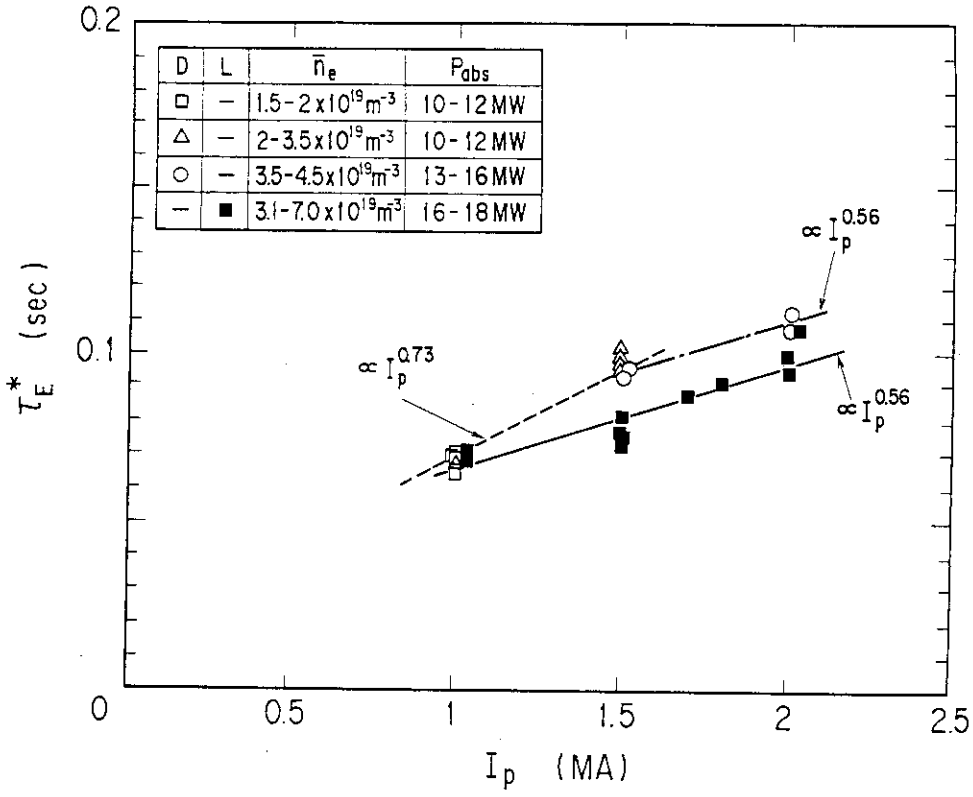

Fig. 6 Plasma current dependence of energy confinement time. Although the radiation losses is high (50~80%) in the limiter discharges, the current dependences of their energy confinement time is shown to be compared with that of the divertor plasmas.

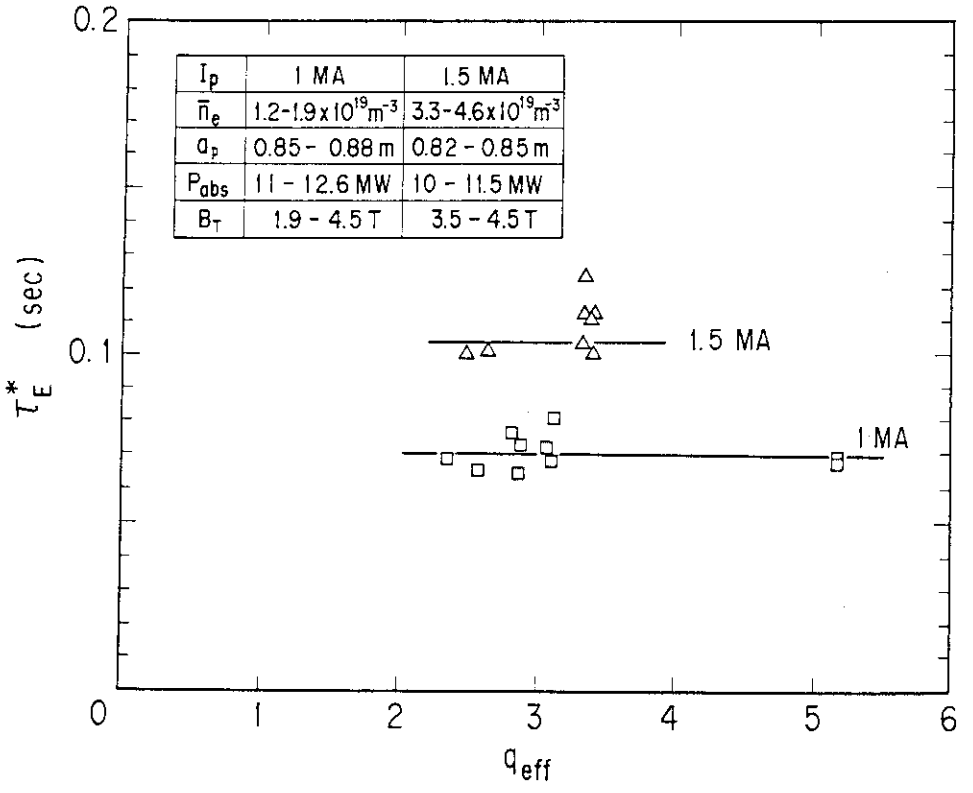

Fig. 7 q_{eff} dependence of energy confinement time.

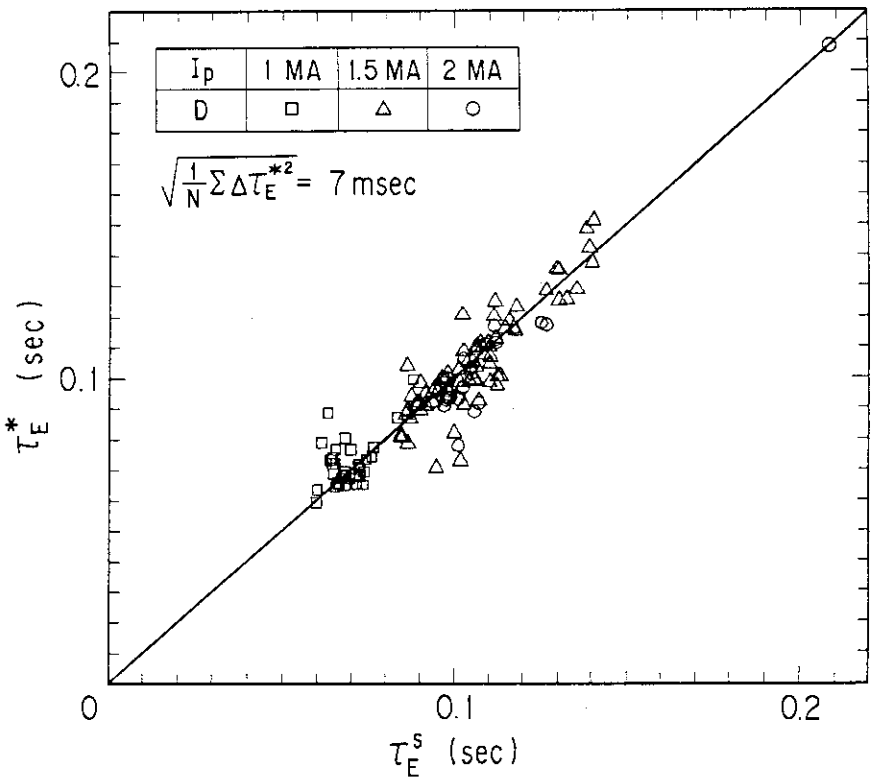

(a) in case of $\tau_E^s(\mathrm{sec}) = (0.033 + 0.37 / P_{abs}(\mathrm{MW}) \times I_p^{0.6}(\mathrm{MA}) n_e^{-0.14}(10^{19}\ \mathrm{m}^{-3})\ q_{eff}^0$

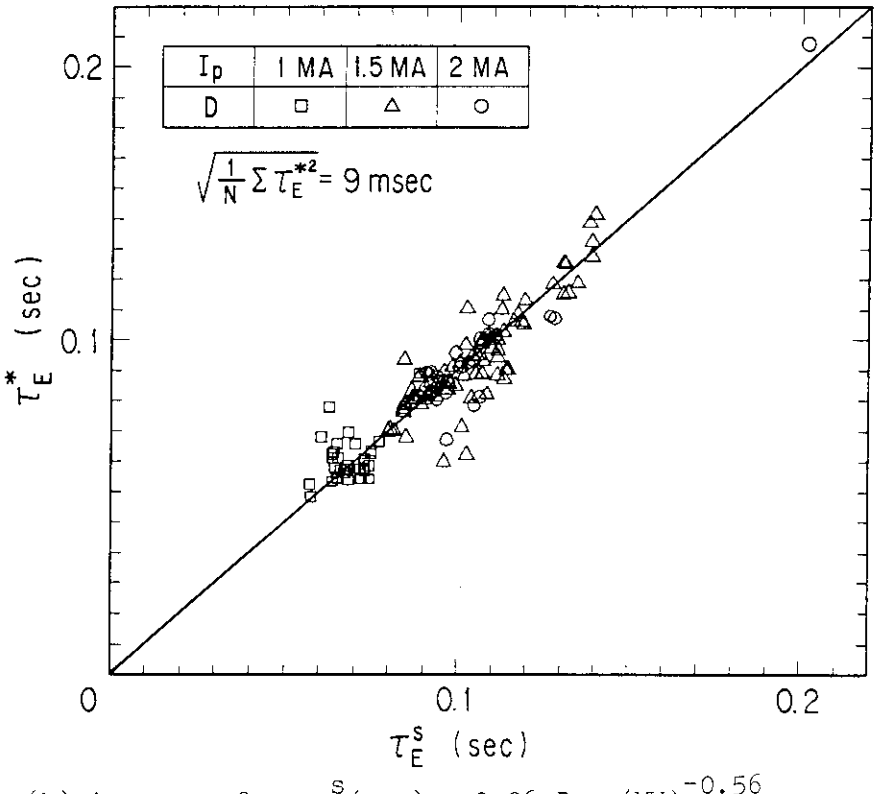

(b) in case of $\tau_E^s(\mathrm{sec}) = 0.26\ P_{abs}(\mathrm{MW})^{-0.56} \times I_p^{0.6}(\mathrm{MA}) n_e^{-0.14}(10^{19}\ \mathrm{m}^{-3})\ q_{eff}^0$

Fig. 8 Comparison of the scaling laws of energy confinement time with the experimental data.